

Article

# (Non-)Thermal Production of WIMPs during Kination

Luca Visinelli 

The Oskar Klein Centre for Cosmoparticle Physics, Department of Physics, Stockholm University, AlbaNova & Nordita, KTH Royal Institute of Technology and Stockholm University, Roslagstullsbacken 23, 10691 Stockholm, Sweden

\* Correspondence: luca.visinelli@fysik.su.se

**Abstract:** Understanding the nature of the Dark Matter (DM) is one of the current challenges in modern astrophysics and cosmology. Knowing the properties of the DM particle would shed light on physics beyond the Standard Model and even provide us with details of the early Universe. In fact, the detection of such a relic would bring us information from the pre-Big Bang Nucleosynthesis (BBN) period, an epoch from which we have no data, and could even hint at inflationary physics. In this work, we assume that the expansion rate of the Universe after inflationary is governed by the kinetic energy of a scalar field  $\phi$ , in the so-called “kination” model. We assume that the  $\phi$  field decays into both radiation and DM particles, which we take to be Weakly Interacting Massive Particles (WIMPs). The present abundance of WIMPs is then fixed during the kination period through either a thermal “freeze-out” or “freeze-in” mechanism, or through a non-thermal process governed by the decay of  $\phi$ . We explore the parameter space of this theory with the requirement that the present WIMP abundance provides the correct DM relic budget. Requiring that BBN occurs during the standard cosmological scenario sets a limit on the temperature at which the kination period ends. Using this limit and assuming the WIMP has a mass  $m_\chi = 100 \text{ GeV}$ , we obtain that the thermally-averaged WIMP annihilation cross section has to satisfy the constraints  $3.5 \times 10^{-16} \text{ GeV}^{-2} \lesssim \langle \sigma v \rangle \lesssim 1.4 \times 10^{-5} \text{ GeV}^{-2}$  in order for having at least one of the production mechanism to yield the observed amount of DM. This result shows how the properties of the WIMP particle, if ever measured, can yield information on the pre-BBN content of the Universe.

**Keywords:** Cosmology; Dark Matter; Early Universe

## 1. Introduction

The existence of a Dark Matter (DM) component in the Universe has long been established [1, 2], with a Weakly Interacting Massive Particle (WIMP) being among the best motivated particle candidates [3,4]. In the simplest scenario of the early Universe, WIMPs of mass  $m_\chi$  interact with the Standard Model (SM) particles at a sufficiently high rate so that the chemical equilibrium is attained. Owing to the expansion rate of the Universe, when the temperature falls below  $T_{\text{chem}} \approx m_\chi/20$  WIMPs chemically decouple from the plasma and “freeze-out” of the equilibrium distribution [5–12]. After freeze-out, the number of WIMPs in a comoving volume is fixed and the WIMP relic abundance is preserved to present day, assuming that there is no subsequent change in the entropy of the matter-radiation fluid. Coincidentally, the thermally-averaged WIMP annihilation cross section needed to explain the observed DM is of the same order of magnitude as that obtained for a process mediated by weakly interactions. For a WIMP of mass  $m_\chi = 100 \text{ GeV}$ , the annihilation cross section that provides the observed amount of DM satisfies  $\langle \sigma v \rangle_{\text{std}} \approx 2 \times 10^{-9} \text{ GeV}^{-2}$ . WIMPs continue to exchange momentum through elastic collisions with the plasma even after chemical decoupling, until this second mechanism also becomes inefficient and WIMPs decouple kinetically at a temperature  $T_{\text{kd}}$ . Typically,  $T_{\text{kd}}$  ranges between 10 MeV and a few GeV [13].

36 Even when considering this thermal production in the standard cosmological scenario, many  
 37 caveats allow to alter the predicted relic density. Besides co-annihilation [14,15], annihilation into  
 38 forbidden channels [14,16,17], a momentum- or spin-dependent cross section [18–20], or Sommerfeld  
 39 enhancement [21–24], one possibility is that the annihilation cross section into the SM sector is so low  
 40 that WIMPs never reach thermal equilibrium, effectively “freezing-in” to the present relic density.  
 41 Examples include models of Feebly Interacting Massive Particles [25–27].

42 WIMPs might also be produced non-thermally, through the decay of a parent particle  $\phi$  [28],  
 43 whose existence is motivated by the post-inflationary reheating scenario. In facts, assume an early  
 44 inflationary stage at an energy scale  $H_I$  driven by one massive scalar field  $\rho$  (the inflaton), of mass  $m_\rho$ .  
 45 When slow-roll is violated, around  $m_\rho \sim H_I$ , inflation ends and the inflaton field reheats the Universe  
 46 by decaying into lighter degrees of freedom [29,30]. We are not entering the details of the reheating  
 47 mechanism here. In the standard picture, a radiation-dominated period begins as soon as the inflaton  
 48 field has decayed and reheated the Universe.

49 However, in some reheating models the inflaton might also decay into one or more additional  
 50 hypothetical fields, say for example a field  $\phi$  of mass  $m_\phi$  which comes to dominate the post-inflationary  
 51 stage. The inclusion of a non-standard cosmology between the reheating epoch right after inflation  
 52 and the standard radiation-dominated scenario is motivated in realistic models of inflation, and might  
 53 sensibly alter the WIMP relic density. A non-standard period might have lasted for a considerable  
 54 amount of time, namely since the end of inflation down to a temperature which, using considerations  
 55 on the Big Bang Nucleosynthesis (BBN) mechanism [31–35], can be as low as  $\sim 5$  MeV. In these  
 56 modified cosmologies, various properties of the WIMPs like their free-streaming velocity and the  
 57 temperature at which the kinetic decoupling occurs have been investigated [36–39].

58 In the Low Temperature Reheat Scenario (LTRS) [40–43],  $\phi$  is a massive modulus which drives  
 59 an early matter-dominated epoch, eventually decaying into Standard Model particles and, possibly,  
 60 WIMPs. In the pre-BBN LTRS, the thermal (both freeze-out and freeze-in) and non-thermal production  
 61 of WIMPs have both been extensively studied [36,44–60].

62 In the Kination Scenario (KS) [61–66],  $\phi$  is a “fast-rolling” field whose kinetic energy governs  
 63 the expansion rate of the post-inflationary Universe, with an equation of state relating the pressure  
 64  $p_\phi$  and energy density  $\rho_\phi$  of the fluid as  $p_\phi = \rho_\phi$ . Owing to the scaling of the energy density in  
 65 radiation with the scale factor  $\rho_R \sim a^{-4}$ , which is slower than the scaling of the energy density in the  $\phi$   
 66 field  $\rho_\phi \sim a^{-6}$ , the contribution from the radiation energy density in determining the expansion rate  
 67 eventually becomes more important than that from the  $\phi$  field. When the  $\phi$  field redshifts away, the  
 68 standard radiation-dominated cosmology takes place. Since the scalar field  $\phi$  dominates the expansion  
 69 rate for some period, KS differs from the superWIMP model of Refs. [67,68]. Thermal production of  
 70 WIMPs in the KS has been discussed in Refs. [65,69–73], and has recently been investigated in Ref. [74],  
 71 in light of recent data. Ref. [75] discussed the “relentless” thermal freeze-out in models where the  $\phi$   
 72 field has a pressure  $p_\phi > \rho_\phi/3$ , thus including KS as an important sub-case. Ref. [76] discusses an  
 73 intermediate model between LTRS and KS, in which a sub-dominant massive scalar field reheats the  
 74 Universe during a kination period governed by an additional field.

75 In this paper, we assume that the  $\phi$  field driving kination might decay into both radiation and  
 76 WIMPs, with a decay rate  $\Gamma_\phi$  and a branching ratio into WIMPs equal to  $b$ . Contrarily to previous KS  
 77 models, kination ends when  $\Gamma_\phi$  is equal to the expansion rate of the Universe, so when the  $\phi$  field  
 78 has decayed instead of being redshifted away. WIMP production proceeds by assuming that, before  
 79 the Universe gets to be dominated by radiation at a temperature  $T_{\text{kin}} \gtrsim 5$  MeV, the KS occurs. In the  
 80 following, the subscript “kin” labels a quantity evaluated at  $T_{\text{kin}}$ . We consider the thermal freeze-out  
 81 and freeze-in mechanisms of WIMP production, governed by the thermal-averaged annihilation cross  
 82 section times velocity  $\langle\sigma v\rangle$ . We also include the non-thermal WIMP production from the decay of the  
 83  $\phi$  field. We check that the WIMP population is always under-abundant with respect to other forms of  
 84 energy. In summary, we show that in the model the present WIMP relic abundance can be reached

85 through four different methods, namely the thermal ( $b = 0$ ) or non-thermal ( $b \neq 0$ ) production, either  
86 with or without ever reaching chemical equilibrium, as occurs in the LTRS [50,51].

## 87 2. Boltzmann equations for the model

88 We follow the evolution of the energy components by modeling the system through a set of  
89 coupled Boltzmann equations

$$\dot{\rho}_\phi + 6H\rho_\phi = -\Gamma_\phi\rho_\phi, \quad (1)$$

$$\dot{\rho}_R + 4H\rho_R = \left(1 - \frac{bm_\chi}{m_\phi}\right)\Gamma_\phi\rho_\phi + \epsilon_\chi\langle\sigma v\rangle(n_\chi^2 - n_{\text{EQ}}^2), \quad (2)$$

$$\dot{n}_\chi + 3Hn_\chi = \frac{b\Gamma_\phi}{m_\phi}\rho_\phi - \langle\sigma v\rangle(n_\chi^2 - n_{\text{EQ}}^2). \quad (3)$$

Here,  $n_\chi$  is the WIMP number density, with a value  $n_{\text{EQ}}$  when in chemical equilibrium,  $\rho_R$  is the energy density in radiation, and we defined the WIMP energy through  $\rho_\chi = \epsilon_\chi n_\chi$ . The equation of state relating the energy density and the pressure of the  $\phi$  field is given by  $\rho_\phi = p_\phi$ , and translates into the term  $6H\rho_\phi$  appearing in Eq. (1). At any time, the temperature  $T$  is defined through the energy density in the relativistic component as  $\rho_R = \alpha T^4$ , with  $\alpha = \pi^2 g_*(T)/30$  and where  $g_*(T)$  is the number of relativistic degrees of freedom. We assume that WIMPs have  $g$  degrees of freedom, so that the equilibrium distribution is given by ( $E^2 = p^2 + m_\chi^2$ )

$$n_{\text{EQ}} = \int f(p) \frac{g d^3 p}{(2\pi)^3} = \frac{g}{2\pi^2} \int_{m_\chi}^{+\infty} \frac{\sqrt{E^2 - m_\chi^2}}{e^{E/T} + 1} E dE. \quad (4)$$

The set of Eqs. (1)-(3) is closed when solved together with the Friedmann equation

$$H^2 = \frac{8\pi}{3M_{\text{Pl}}^2} (\rho_\phi + \rho_R + m_\chi n_\chi), \quad (5)$$

90 where  $M_{\text{Pl}}$  is the Planck mass. We assume that the mass of the  $\phi$  field is larger than both  $\epsilon_\chi$  and  $bm_\chi$ .  
91 In this limit, Eqs. (1)-(3) simplify as

$$\dot{\rho}_\phi + 6H\rho_\phi = -\Gamma_\phi\rho_\phi, \quad (6)$$

$$\dot{\rho}_R + 4H\rho_R = \Gamma_\phi\rho_\phi, \quad (7)$$

$$\dot{n}_\chi + 3Hn_\chi = \frac{b\Gamma_\phi}{m_\phi}\rho_\phi - \langle\sigma v\rangle(n_\chi^2 - n_{\text{EQ}}^2). \quad (8)$$

At early times  $t \ll 1/\Gamma_\phi$ , the Boltzmann Eq. (6) and the Friedmann Eq. (5) predict that, during KS, the energy density of the  $\phi$  field and time scale as  $\rho_\phi \sim a^{-6}$  and  $t \sim a^3$ , respectively. Contrarily to what found in kination models with negligible decay rate, for which  $a \sim 1/T$  [63–66], in the model we study temperature depends on the scale factor as  $T \propto \rho_\phi^{1/8} \propto a^{-3/4}$ . In more details, Eq. (7) can be reformulated as a differential equation describing the evolution of the entropy per comoving volume  $s = (p_R + \rho_R)/T$ , as

$$\frac{ds}{dt} + 3Hs = \frac{\Gamma_\phi}{T}\rho_\phi. \quad (9)$$

92 As a consequence, entropy is not conserved in the model we consider because of the appearance of  
93 the dissipative term on the right hand side in Eq. (9), coming from the decay of the  $\phi$  field. We later  
94 confirm these results by numerically solving the set of the Boltzmann equations, see Fig. 1 below.

We switch to the independent coordinates  $x = m_\phi a$  and  $\tau = \Gamma_\phi t$ , while we write the dependent quantities in terms of the fields

$$\Phi = Ax^6 \rho_\phi / m_\phi, \quad R = Ax^4 \rho_R / m_\phi, \quad X = Ax^3 n_\chi. \quad (10)$$

Fixing the constant  $A$  through the Friedmann equation,

$$\mathcal{H} = \frac{1}{x} \frac{dx}{d\tau} = \frac{H}{\Gamma_\phi} = \frac{\sqrt{\Phi + Rx^2 + x^3 X}}{x^3}, \quad (11)$$

we obtain that Eq. (5) is recovered when

$$A = \frac{8\pi m_\phi}{3M_{\text{Pl}}^2 \Gamma_\phi^2} \equiv \frac{m_\phi}{\rho_{\text{kin}}}, \quad (12)$$

95 where we have defined the temperature  $T_{\text{kin}}$  in the instantaneous thermalization approximation,  
96  $\rho_{\text{kin}} = \rho_R(T_{\text{kin}})$ , so that  $\Gamma_\phi = H(T_{\text{kin}})$ . With this definition, we rewrite the system of Eqs. (6)-(8) as

$$\Phi' = \frac{-x^2 \Phi}{\sqrt{\Phi + x^2 R + x^3 X'}} \quad (13)$$

$$R' = \frac{\Phi}{\sqrt{\Phi + x^2 R + x^3 X'}} \quad (14)$$

$$X' = \frac{b\Phi - s(X^2 - X_{\text{EQ}}^2)}{x\sqrt{\Phi + x^2 R + x^3 X'}} \quad (15)$$

where  $s = \langle \sigma v \rangle / \Gamma_\phi A = \rho_{\text{kin}} \langle \sigma v \rangle / \Gamma_\phi m_\phi$ . This dimensionless form of the system has never been shown in the literature, and can be easily extended to cosmologies other than KS. We assume that the relativistic species is always at equilibrium, so that temperature is related to  $R$  as  $T = T_{\text{kin}} R^{1/4} / x$ . At chemical equilibrium, the quantity  $X_{\text{EQ}} = Ax^3 n_{\text{EQ}}$  is then

$$X_{\text{EQ}} = \frac{gm_\phi}{\rho_{\text{kin}}} \left( \frac{m_\chi T_{\text{kin}} x R^{1/4}}{2\pi} \right)^{3/2} \exp\left( \frac{-m_\chi x}{T_{\text{kin}} R^{1/4}} \right). \quad (16)$$

The set of Eqs. (13)-(16) possesses a scaling symmetry,

$$x \rightarrow \beta x, \quad \Phi \rightarrow \beta^6 \Phi, \quad R \rightarrow \beta^4 R, \quad X \rightarrow \beta^3 X, \quad (17)$$

for any value of  $\beta$ , thanks to which the solution to the set of Boltzmann equations is independent on choice of the initial value  $\Phi(x_I) = \Phi_I$  at  $x = x_I$  [45,46]. We fix the initial condition by requiring that the Hubble rate at  $x = x_I$  be  $H_I = \sqrt{8\pi\rho_I/3M_{\text{Pl}}^2}$ , where  $\rho_I$  is the value of the energy density in the inflaton field at the inflation scale. Indeed, assuming that  $\rho_R(x_I) \ll \rho_\phi(x_I) \equiv \rho_I$  gives

$$\Phi(x) = \Phi_I \equiv \frac{\rho_I}{\rho_{\text{kin}}} x_I^6, \quad R(x) = \sqrt{\Phi_I} (x - x_I). \quad (18)$$

Since the energy density  $\rho_\phi$  during  $\phi$ -domination satisfies  $\rho_\phi \sim a^{-6}$ , the transition to the standard radiation-dominated scenario occurs when

$$\rho_{\phi,I} \left( \frac{x_I}{x_{\text{kin}}} \right)^6 = \rho_{\text{kin}} \equiv \alpha T_{\text{kin}}^4. \quad (19)$$

97 Given the value of  $T_{\text{kin}}$ , Eq. (19) defines the moment at which the  $\phi$  field decays. For the illustrative  
98 purpose, we solve Eqs. (13) and (14) for  $T_{\text{kin}} = 0.1 \text{ GeV}$ , fixing the masses  $m_\chi = 100 \text{ GeV}$  and  $m_\phi =$

99 1000 TeV and assuming that we can safely neglect the contribution of WIMPs to the total energy density.  
 100 We have plot  $\Phi$  (blue solid line) and  $R$  (red dashed line) in units of  $\Phi_I$ , as well as the temperature  $T/T_I$   
 101 (black dot-dashed line). The behavior of  $\Phi$  confirms the scaling  $\rho_\phi \sim a^{-6}$  and  $\rho_R \sim a^{-3}$  at early times  
 102  $x < x_{\text{kin}}$ , while for  $x > x_{\text{kin}}$  we obtain the scaling  $\rho_R \sim a^{-4}$  for a radiation-dominated cosmology. The  
 dashed vertical line marks the value of  $x_{\text{kin}}$  solution to Eq. (19).

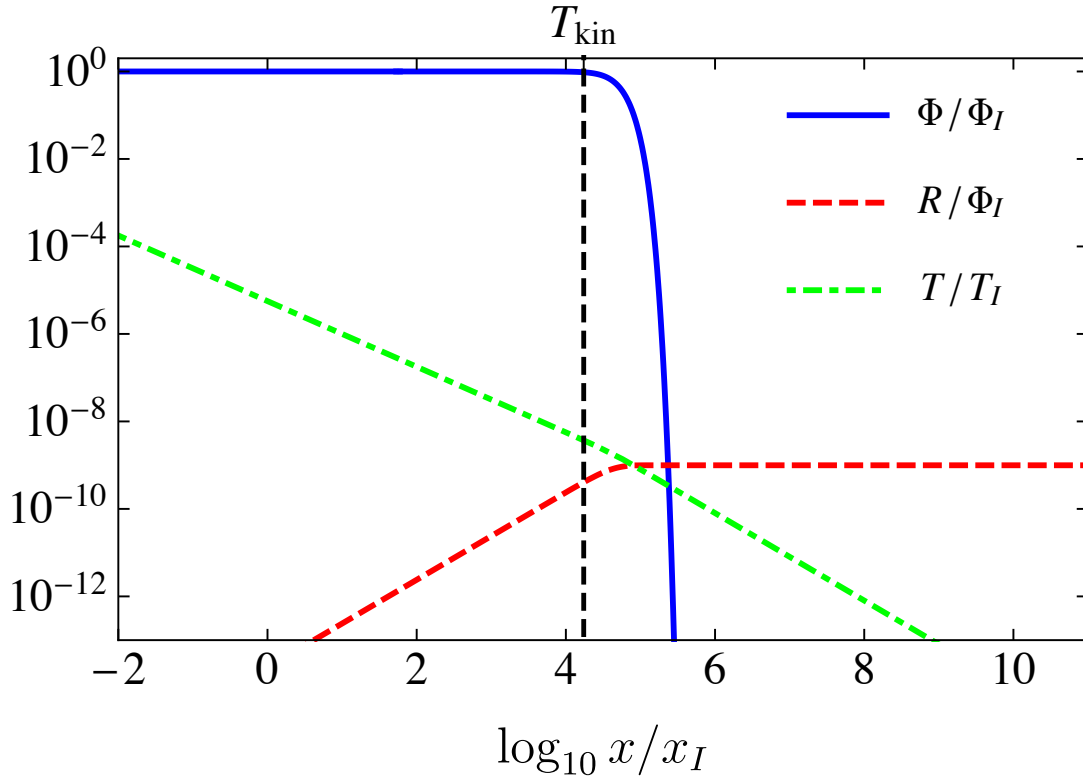


**Figure 1.** The quantities  $\Phi$  and  $R$ , defined in Eq. (10) and related to  $\rho_\phi$  and  $\rho_R$  respectively, in units of the initial value  $\Phi_I$ . The vertical dashed line marks the moment at which the transition to the standard scenario occurs, according to Eq. (19). The green dot-dashed line shows the temperature  $T(x)$ , in units of its initial value  $T(x_I)$ .

103

### 104 3. Production of WIMPs during kination

With this framework, we solve the set of Boltzmann Eqs. (13)-(15) for different values of  $T_{\text{kin}}$ , to obtain the WIMP relic abundance  $n_{\text{kin}} \equiv n_\chi(T_{\text{kin}})$  when the  $\phi$  field decays, after which the WIMP number density in a comoving volume is fixed. The present WIMP energy density in units of the critical density  $\rho_c$  is then

$$\Omega_\chi = \frac{m_\chi}{m_\phi} \frac{\rho_{\text{kin}}}{\rho_c} \frac{g_S(T_0)}{g_S(T_{\text{kin}})} \left( \frac{T_0}{T_{\text{kin}}} \right)^3 \frac{X_{\text{kin}}}{\sqrt{\Phi_I}}, \quad (20)$$

105 where  $X_{\text{kin}} = A x_{\text{kin}}^3 n_{\text{kin}}$ ,  $T_0$  is the present temperature of the radiation bath and  $g_S(T)$  is the number  
 106 of entropy degrees of freedom at temperature  $T$ . We show different values of the abundance  $\Omega_\chi h^2$  in  
 107 Fig. 2, as a function of the temperature  $T_{\text{kin}}$ , the annihilation cross section  $\langle \sigma v \rangle$ , and the branching ratio  
 108  $b$ . We have used three different values of  $b = 10^{-10}$ ,  $10^{-5}$ , and  $10^{-1}$ , as well as five different values  
 109 of  $\langle \sigma v \rangle$ . The value  $\langle \sigma v \rangle = \langle \sigma v \rangle_{\text{std}}$  gives the correct amount of DM when  $T_{\text{kin}} \gtrsim m_\chi/20$ , since in such  
 110 scenario the chemical decoupling of WIMPs occurs in the standard cosmology. The extra dashed line  
 111 at  $T_{\text{kin}} = 0.1$  GeV tracks the specific solution of the Boltzmann equations later used in Fig. 3. The value

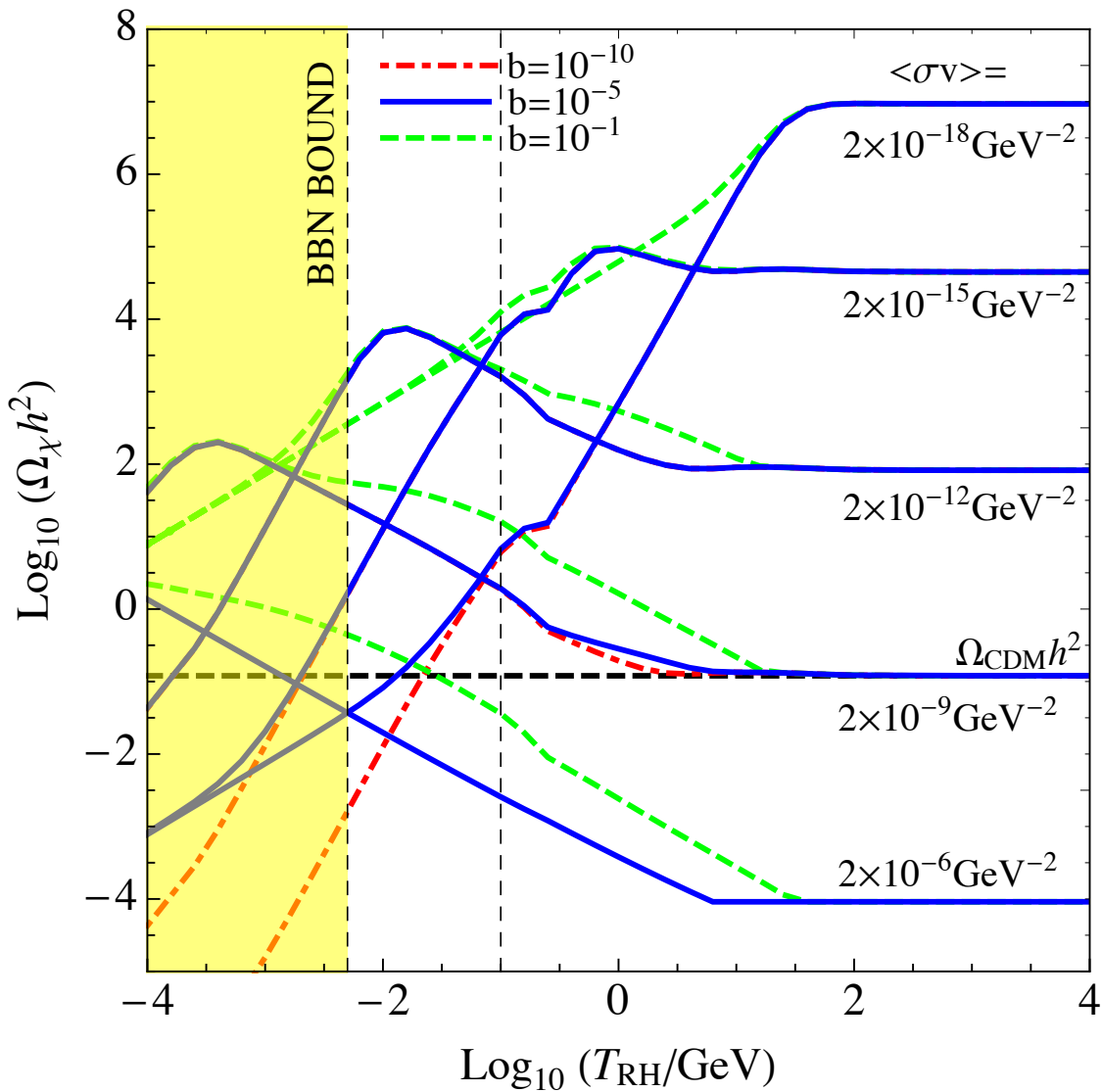


**Figure 2.** The present WIMP relic abundance for different values of  $\langle\sigma v\rangle$  (see figure labels), and for different values of the branching ratio:  $b = 10^{-10}$  (red dot-dashed line),  $b = 10^{-5}$  (blue solid line), and  $b = 10^{-1}$  (green dashed line), as a function of  $T_{\text{kin}}$ . The horizontal dashed line shows the measured dark matter abundance  $\Omega_{\text{DM}}h^2 \sim 0.12$ . The vertical yellow band defines the region excluded by BBN considerations,  $T_{\text{kin}} \geq 5 \text{ MeV}$ . The vertical line at  $T_{\text{kin}} = 0.1 \text{ GeV}$  marks the solutions to the Boltzmann Eq. (15) later used for Fig. 3, using  $b = 0.1$ .

<sup>112</sup> of  $n_{\text{kin}}$  depends on the specific mechanism that dominates the production of the WIMP population.  
<sup>113</sup> According to the values of  $b$  and  $\langle\sigma v\rangle$ , four possibilities appear, namely:

- Thermal production with chemical equilibrium (“freeze-out”, Mechanism 1). We first focus on the case  $b = 0$ , corresponding to the negligible decay with respect to the annihilation into standard model particles and approximated by the red dot-dashed and blue solid lines in Fig. 2.

We assume that the temperature  $T_{\text{kin}}$  is lower than the freeze-out temperature  $T_{\text{f.o.}}$ , which is defined as the temperature at which  $n\langle\sigma v\rangle = H$ , or

$$n_{\text{EQ}}(T_{\text{f.o.}}) = \left(\frac{T_{\text{f.o.}}}{T_{\text{kin}}}\right)^4 \frac{H(T_{\text{kin}})}{\langle\sigma v\rangle}. \quad (21)$$

However, contrary to what obtained in the standard radiation-dominated scenario, the WIMP number density in the kination cosmology is not fixed at  $T_{\text{f.o.}}$  and annihilation continues until the temperature drops to  $T_{\text{kin}}$  and the expansion rate transitions to that of a radiation-dominated one [75]. We assume that the freeze-out is reached at  $x_{\text{f.o.}}$ , for which  $X(x_{\text{f.o.}}) = X_{\text{f.o.}}$ . For later times, using the approximation in Eq. (19), Eq. (15) reduces to

$$X' = -\frac{\rho_{\text{kin}}\langle\sigma v\rangle}{\Gamma_{\phi}m_{\phi}} \frac{X^2}{x\sqrt{\Phi_I}}, \quad (22)$$

whose solution at  $x > x_{\text{f.o.}}$  give the abundance of thermally produced WIMPs at  $T_{\text{kin}}$ , which reads

$$X_{\text{kin,th}} = \left[ \frac{1}{X_{\text{f.o.}}} + \frac{\langle\sigma v\rangle T_{\text{kin}}^2}{\sqrt{\Phi_I}} \frac{M_{\text{Pl}}}{m_{\phi}} \ln \frac{x_{\text{kin}}}{x_{\text{fo}}} \right]^{-1}. \quad (23)$$

Neglecting  $X_{\text{f.o.}}$ , the present abundance in Eq. (20) for the standard freeze-out mechanism gives

$$\Omega_{\chi} = \frac{g_S(T_0)}{g_S(T_{\text{kin}})} \frac{m_{\chi}}{M_{\text{Pl}}} \frac{\rho_{\text{kin}}}{\rho_c} \frac{T_0^3}{\langle\sigma v\rangle T_{\text{kin}}^5} \left( \ln \frac{x_{\text{kin}}}{x_{\text{fo}}} \right)^{-1} \propto \frac{1}{T_{\text{kin}}}. \quad (24)$$

114 The solution describes the lines with negative slopes in Fig. 2, for  $b = 10^{-10}$  and  $b = 10^{-5}$  and for  
115 the cross sections  $\langle\sigma v\rangle = 2 \times 10^{-6} \text{ GeV}^{-2}$ ,  $\langle\sigma v\rangle = 2 \times 10^{-9} \text{ GeV}^{-2}$ , and  $\langle\sigma v\rangle = 2 \times 10^{-12} \text{ GeV}^{-2}$ .

- Thermal production without ever reaching chemical equilibrium (“freeze-in”, Mechanism 2). If the cross section is sufficiently low [74], WIMPs never reach thermal equilibrium and their number density freezes in at a fixed quantity. Since the number density of particles is always smaller than their value at thermal equilibrium, we neglect  $X \ll X_{\text{EQ}}$  so Eq. (15) with  $b = 0$  reads

$$X' = \frac{\rho_{\text{kin}}\langle\sigma v\rangle}{\Gamma_{\phi}m_{\phi}} \frac{(X_{\text{EQ}}^2)}{x\sqrt{\Phi_I}} = c_1 x^{11/4} \exp(-2c_2 x^{3/4}), \quad (25)$$

where

$$c_1 = \frac{g^2\langle\sigma v\rangle m_{\phi} m_{\chi}^3 T_{\text{kin}}^3}{(2\pi)^3 \Gamma_{\phi} \rho_{\text{kin}} \Phi_I^{1/8}}, \quad \text{and} \quad c_2 = \frac{m_{\chi}}{T_{\text{kin}} \Phi_I^{1/8}}. \quad (26)$$

The solution to Eq. (25) reaches the asymptotic value of  $X$  at freeze-in

$$X_{\text{kin,fi}} = \frac{c_1}{c_2^5} = \frac{g^2\langle\sigma v\rangle m_{\phi} T_{\text{kin}}^8 \sqrt{\Phi_I}}{(2\pi)^3 \Gamma_{\phi} \rho_{\text{kin}} m_{\chi}^2}, \quad (27)$$

which is reached when  $x_{\text{fi}} = (6/11c_2)^{4/3}$ . The present abundance is then

$$\Omega_{\chi} = \frac{g_S(T_0)}{g_S(T_{\text{kin}})} \frac{g^2\langle\sigma v\rangle T_0^3 T_{\text{kin}}^5}{(2\pi)^3 \Gamma_{\phi} \rho_c m_{\chi}} \propto T_{\text{kin}}^3. \quad (28)$$

116 The solution describes the lines with positive slopes in Fig. 2, for  $b = 10^{-10}$  and  $b = 10^{-5}$   
117 and for the cross sections  $\langle\sigma v\rangle = 2 \times 10^{-12} \text{ GeV}^{-2}$ ,  $\langle\sigma v\rangle = 2 \times 10^{-15} \text{ GeV}^{-2}$ , and  $\langle\sigma v\rangle =$   
118  $2 \times 10^{-18} \text{ GeV}^{-2}$ .

- Non-thermal production without chemical equilibrium (Mechanism 3). We now discuss the non-thermal production of dark matter, in the case in which the particle has never reached

the chemical equilibrium. For a large branching ratio  $b = O(0.1)$ , and for  $T_{\text{kin}} \ll m_\chi$ , the abundance of dark matter is set by the decay of the  $\phi$  field, with a number density at  $T_{\text{kin}}$  given by [50,52,55,58,60,77]

$$n_{\text{kin}} \approx b n_\phi(T_{\text{kin}}) = b \frac{\rho_{\text{kin}}}{m_\phi}. \quad (29)$$

Deriving the result from directly integrating Eq. (15) with  $\langle\sigma v\rangle = 0$  and neglecting the contributions from  $R$  and  $X$  in the denominator gives an extra logarithmic dependence on  $x_{\text{kin}}$ , as

$$X_{\text{kin,decay}} = b \sqrt{\Phi_I} \ln \frac{x_{\text{kin}}}{x_I}. \quad (30)$$

119 The present WIMP abundance when the non-thermal production dominates is given by Eq. (20)  
 120 with  $X_{\text{kin}}$  as in Eq. (30), and predicts the behavior  $\Omega_\chi \propto T_{\text{kin}}$  corresponding to the green dashed  
 121 line with  $\langle\sigma v\rangle = 10^{-18} \text{ GeV}^{-2}$  in Fig. 2, for  $T_{\text{kin}} \lesssim 10 \text{ GeV}$ . Notice that, except for the logarithmic  
 122 dependence which is present in the kination cosmology, the result in Eq. (30) is independent of  
 123 the cosmology used, so the result in Eq. (29) also holds in the LTRS.

- Non-thermal production with chemical equilibrium (Mechanism 4). If the branching ratio  $b$  is sufficiently high, we find that the quantity  $X$  is fixed to the value at freeze-out, which is obtained by setting to zero the right-hand side of Eq. (15),

$$X_{\text{kin,ann}} = \sqrt{\frac{b\Phi_I\Gamma_\phi m_\phi}{\rho_{\text{kin}}\langle\sigma v\rangle}}. \quad (31)$$

The result in Eq. (31) can be alternatively derived by considering the balancing between the decay rate of the  $\phi$  field into WIMPs and the annihilation rate of WIMPs, as

$$\langle\sigma v\rangle n_\chi^2 = b\Gamma_\phi \frac{\rho_\phi}{m_\phi}. \quad (32)$$

The value of  $X_{\text{kin,ann}}$  remains constant until  $T_{\text{kin}}$ , without experiencing the additional depletion described in the freeze-out regime [74,75]. However, when the temperature of the plasma falls below  $T_{\text{kin}}$ , the energy density in the  $\phi$  field drops to zero, while WIMP annihilation is still maintained approximately until  $\rho_\phi \approx \rho_R$ , when the WIMP number density is

$$n_\chi = \frac{\Gamma_\phi}{\langle\sigma v\rangle}, \quad \text{or} \quad X_{\text{kin,nonTH}} = \sqrt{\frac{b\rho_{\text{kin}}\langle\sigma v\rangle}{\Gamma_\phi m_\phi}} \quad (33)$$

The present abundance is expressed as

$$\Omega_\chi = \frac{m_\chi \Gamma_\phi}{\rho_c \langle\sigma v\rangle} \frac{g_S(T_0)}{g_S(T_{\text{kin}})} \left( \frac{T_0}{T_{\text{kin}}} \right)^3 \propto \frac{1}{T_{\text{kin}}}. \quad (34)$$

#### 124 4. Discussion and summary

In Fig. 3, we summarize the results obtained by considering the behavior of the quantity  $X$  solution to the Boltzmann Eq. (15) for  $b = 0.1$ , the green dot-dashed line in Fig. 2, and for  $T_{\text{kin}} = 0.1 \text{ GeV}$ . In facts, for this choice of the parameters, the different values of  $\langle\sigma v\rangle$  in Fig. 2 give the different production mechanisms discussed. In Fig. 3, the black solid line represents  $X_{\text{EQ}}$ , while the different mechanisms of productions are all given for different values of  $\langle\sigma v\rangle$ , with  $\langle\sigma v\rangle = 2 \times 10^{-9} \text{ GeV}^{-2}$  (blue line) describing non-thermal production with chemical equilibrium (Mechanism 4),  $\langle\sigma v\rangle = 2 \times 10^{-18} \text{ GeV}^{-2}$  (green line) describing non-thermal production without chemical equilibrium (Mechanism 3),  $\langle\sigma v\rangle = 2 \times 10^{-15} \text{ GeV}^{-2}$  (orange line) describing thermal production without chemical equilibrium (Mechanism 2), and  $\langle\sigma v\rangle = 2 \times 10^{-12} \text{ GeV}^{-2}$  (red line) describing thermal production with chemical equilibrium



(Mechanism 1). In addition to the thermal mechanisms of production recently discussed in Refs. [74,75],

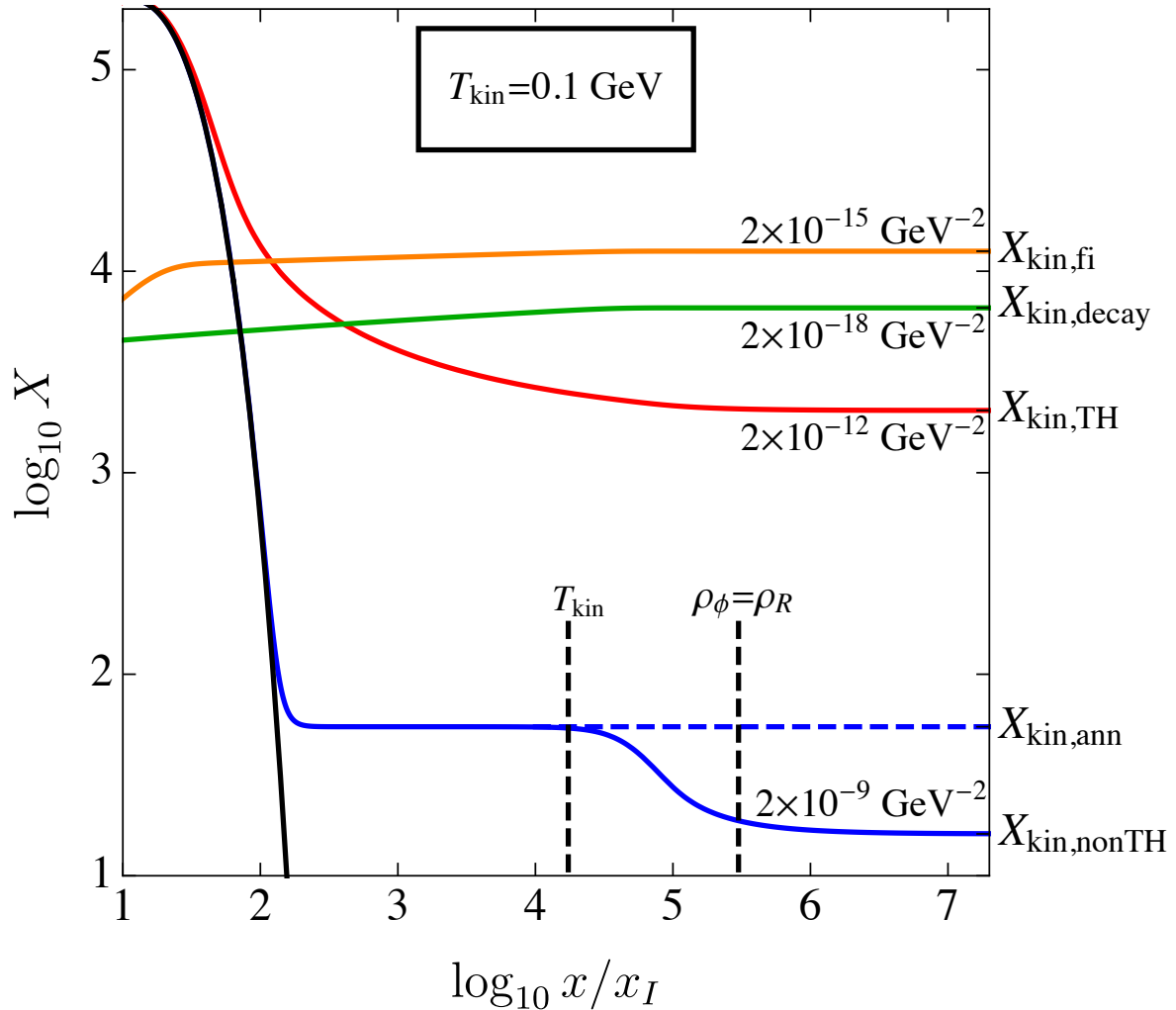


**Figure 3.** The solution to the Boltzmann Eq. (15) for different values of the annihilation cross section. We have set  $T_{\text{kin}} = 0.1$  GeV and, when non-thermal production is considered,  $b = 0.1$ . See text for further details.

we have included the possibility that the field  $\phi$  responsible for the kination period decays into radiation and WIMPs. We have then studied the non-thermal production of WIMPs in the kination cosmology, as summarized in Fig. 2. Given the value  $\langle\sigma v\rangle_{\text{std}} = 2 \times 10^{-9} \text{ GeV}^{-2}$  that gives the present abundance of DM from the freeze-out of WIMPs in the standard cosmology, Fig. 2 shows that larger values of  $\langle\sigma v\rangle$  can still lead to the right DM abundance, if WIMPs are produced either through Mechanisms 1) or 4) during the KS. Similarly, we can have  $\langle\sigma v\rangle$  smaller than its standard value and still have the correct amount of DM, if WIMPs are produced through Mechanism 2). Non-thermal production without chemical equilibrium (Mechanism 3) would lead to the correct amount of DM only for values of  $T_{\text{kin}}$  that are excluded by the BBN considerations. Using the bound  $T_{\text{kin}} \gtrsim 5 \text{ MeV}$ , we infer the possible range of the parameter

$$3.5 \times 10^{-16} \text{ GeV}^{-2} \lesssim \langle\sigma v\rangle \lesssim 1.4 \times 10^{-5} \text{ GeV}^{-2}, \quad (35)$$

125 the lower bound being obtained by using Mechanism 2 and the upper bound being given by  
126 Mechanism 4 with  $b = 1$ . This result is valid for a WIMP of mass  $m_\chi = 100$  GeV and  $m_\phi = 1000$  TeV.

127 To summarize, if the DM is a WIMP of mass  $m_\chi = 100$  GeV, and if the annihilation cross section is  
128 measured to lie outside of the bound in Eq. (35), then the kination model discussed would have to be  
129 discarded. The same analysis can be performed by varying the masses of the WIMP and of the  $\phi$  field,  
130 which would lead to different values of the bounds in Eq. (35). If ever discovered, the properties of the  
131 WIMP could then shed light on the pre-BBN cosmology.

132 **Acknowledgments:** We thank Adrienne Erickcek, Kayla Redmond, and Sunny Vagnozzi for reading earlier  
133 versions of the manuscript. We acknowledge support by the Vetenskapsrådet (Swedish Research Council) through  
134 contract No. 638-2013-8993 and the Oskar Klein Centre for Cosmoparticle Physics.

135 **Conflicts of Interest:** The authors declare no conflict of interest. The founding sponsors had no role in the design  
136 of the study; in the collection, analyses, or interpretation of data; in the writing of the manuscript, and in the  
137 decision to publish the results.

### 138 Abbreviations

139 The following abbreviations are used in this manuscript:

140

DM	Dark Matter
BBN	Big Bang Nucleosynthesis
141 WIMP	Weakly Interacting Massive Particle
LTRS	Low Temperature Reheat Scenario
KS	Kination Scenario

142

- 143 1. Ade, P.A.R.; others. Joint Analysis of BICEP2/Keck Array and Planck Data. *Phys. Rev. Lett.* **2015**,  
144 *114*, 101301, [[arXiv:astro-ph/1502.00612](https://arxiv.org/abs/astro-ph/1502.00612)].
- 145 2. Ade, P.A.R.; others. Planck 2015 results. XIII. Cosmological parameters. *Astron. Astrophys.* **2016**, *594*, A13,  
146 [[arXiv:astro-ph/1502.01589](https://arxiv.org/abs/astro-ph/1502.01589)].
- 147 3. Jungman, G.; Kamionkowski, M.; Griest, K. Supersymmetric dark matter. *Phys. Rept.* **1996**, *267*, 195–373,  
148 [[arXiv:hep-ph/9506380](https://arxiv.org/abs/hep-ph/9506380)].
- 149 4. Bertone, G.; Hooper, D.; Silk, J. Particle dark matter: Evidence, candidates and constraints. *Phys. Rept.*  
150 **2005**, *405*, 279–390, [[arXiv:hep-ph/0404175](https://arxiv.org/abs/hep-ph/0404175)].
- 151 5. Vysotsky, M.I.; Dolgov, A.D.; Zeldovich, Ya.B. Cosmological Restriction on Neutral Lepton Masses. *JETP*  
152 *Lett.* **1977**, *26*, 188–190. [Pisma Zh. Eksp. Teor. Fiz.26,200(1977)].
- 153 6. Hut, P. Limits on Masses and Number of Neutral Weakly Interacting Particles. *Phys. Lett.* **1977**, *69B*, 85.
- 154 7. Sato, K.; Kobayashi, M. Cosmological Constraints on the Mass and the Number of Heavy Lepton Neutrinos.  
155 *Prog. Theor. Phys.* **1977**, *58*, 1775.
- 156 8. Lee, B.W.; Weinberg, S. Cosmological Lower Bound on Heavy Neutrino Masses. *Phys. Rev. Lett.* **1977**,  
157 *39*, 165–168.
- 158 9. Dicus, D.A.; Kolb, E.W.; Teplitz, V.L. Cosmological Implications of Massive, Unstable Neutrinos: New and  
159 Improved. *Astrophys. J.* **1978**, *221*, 327–341.
- 160 10. Steigman, G. Cosmology Confronts Particle Physics. *Ann. Rev. Nucl. Part. Sci.* **1979**, *29*, 313–338.
- 161 11. Bernstein, J.; Brown, L.S.; Feinberg, G. The Cosmological Heavy Neutrino Problem Revisited. *Phys. Rev.*  
162 **1985**, *D32*, 3261.
- 163 12. Kolb, E.W.; Olive, K.A. The Lee-Weinberg Bound Revisited. *Phys. Rev.* **1986**, *D33*, 1202. [Erratum: *Phys.*  
164 *Rev.*D34,2531(1986)].
- 165 13. Profumo, S.; Sigurdson, K.; Kamionkowski, M. What mass are the smallest protohalos? *Phys. Rev. Lett.*  
166 **2006**, *97*, 031301, [[arXiv:astro-ph/0603373](https://arxiv.org/abs/astro-ph/0603373)].
- 167 14. Griest, K.; Seckel, D. Three exceptions in the calculation of relic abundances. *Phys. Rev.* **1991**,  
168 *D43*, 3191–3203.

- 169 15. Edsjo, J.; Gondolo, P. Neutralino relic density including coannihilations. *Phys. Rev.* **1997**, *D56*, 1879–1894,  
170 [arXiv:hep-ph/hep-ph/9704361].
- 171 16. D’Agnolo, R.T.; Ruderman, J.T. Light Dark Matter from Forbidden Channels. *Phys. Rev. Lett.* **2015**,  
172 *115*, 061301, [arXiv:hep-ph/1505.07107].
- 173 17. Cline, J.; Liu, H.; Slatyer, T.; Xue, W. Enabling Forbidden Dark Matter. *Phys. Rev.* **2017**, *D96*, 083521,  
174 [arXiv:hep-ph/1702.07716].
- 175 18. Chang, S.; Pierce, A.; Weiner, N. Momentum Dependent Dark Matter Scattering. *JCAP* **2010**, *1001*, 006,  
176 [arXiv:hep-ph/0908.3192].
- 177 19. Fan, J.; Reece, M.; Wang, L.T. Non-relativistic effective theory of dark matter direct detection. *JCAP* **2010**,  
178 *1011*, 042, [arXiv:hep-ph/1008.1591].
- 179 20. Fitzpatrick, A.L.; Haxton, W.; Katz, E.; Lubbers, N.; Xu, Y. The Effective Field Theory of Dark Matter Direct  
180 Detection. *JCAP* **2013**, *1302*, 004, [arXiv:hep-ph/1203.3542].
- 181 21. Cirelli, M.; Kadastik, M.; Raidal, M.; Strumia, A. Model-independent implications of the  $e^+$ , anti-proton  
182 cosmic ray spectra on properties of Dark Matter. *Nucl. Phys.* **2009**, *B813*, 1–21, [arXiv:hep-ph/0809.2409].  
183 [Addendum: *Nucl. Phys.*B873,530(2013)].
- 184 22. Arkani-Hamed, N.; Finkbeiner, D.P.; Slatyer, T.R.; Weiner, N. A Theory of Dark Matter. *Phys. Rev.* **2009**,  
185 *D79*, 015014, [arXiv:hep-ph/0810.0713].
- 186 23. Pospelov, M.; Ritz, A. Astrophysical Signatures of Secluded Dark Matter. *Phys. Lett.* **2009**, *B671*, 391–397,  
187 [arXiv:hep-ph/0810.1502].
- 188 24. Fox, P.J.; Poppitz, E. Leptophilic Dark Matter. *Phys. Rev.* **2009**, *D79*, 083528, [arXiv:hep-ph/0811.0399].
- 189 25. Hall, L.J.; Jedamzik, K.; March-Russell, J.; West, S.M. Freeze-In Production of FIMP Dark Matter. *JHEP*  
190 **2010**, *03*, 080, [arXiv:hep-ph/0911.1120].
- 191 26. Co, R.T.; D’Eramo, F.; Hall, L.J.; Pappadopulo, D. Freeze-In Dark Matter with Displaced Signatures at  
192 Colliders. *JCAP* **2015**, *1512*, 024, [arXiv:hep-ph/1506.07532].
- 193 27. Bernal, N.; Heikinheimo, M.; Tenkanen, T.; Tuominen, K.; Vaskonen, V. The Dawn of FIMP Dark Matter: A  
194 Review of Models and Constraints. *Int. J. Mod. Phys.* **2017**, *A32*, 1730023, [arXiv:hep-ph/1706.07442].
- 195 28. Kamionkowski, M.; Turner, M.S. Thermal relics: Do we know their abundances? *Phys. Rev. D* **1990**,  
196 *42*, 3310–3320.
- 197 29. Kofman, L.; Linde, A.D.; Starobinsky, A.A. Reheating after inflation. *Phys. Rev. Lett.* **1994**, *73*, 3195–3198,  
198 [arXiv:hep-th/hep-th/9405187].
- 199 30. Kofman, L.; Linde, A.D.; Starobinsky, A.A. Towards the theory of reheating after inflation. *Phys. Rev.* **1997**,  
200 *D56*, 3258–3295, [arXiv:hep-ph/hep-ph/9704452].
- 201 31. Kawasaki, M.; Kohri, K.; Sugiyama, N. Cosmological constraints on late time entropy production. *Phys.*  
202 *Rev. Lett.* **1999**, *82*, 4168, [arXiv:astro-ph/astro-ph/9811437].
- 203 32. Kawasaki, M.; Kohri, K.; Sugiyama, N. MeV scale reheating temperature and thermalization of neutrino  
204 background. *Phys. Rev.* **2000**, *D62*, 023506, [arXiv:astro-ph/astro-ph/0002127].
- 205 33. Hannestad, S. What is the lowest possible reheating temperature? *Phys. Rev.* **2004**, *D70*, 043506,  
206 [arXiv:astro-ph/astro-ph/0403291].
- 207 34. Ichikawa, K.; Kawasaki, M.; Takahashi, F. The Oscillation effects on thermalization of the  
208 neutrinos in the Universe with low reheating temperature. *Phys. Rev.* **2005**, *D72*, 043522,  
209 [arXiv:astro-ph/astro-ph/0505395].
- 210 35. De Bernardis, F.; Pagano, L.; Melchiorri, A. New constraints on the reheating temperature of the universe  
211 after WMAP-5. *Astropart. Phys.* **2008**, *30*, 192–195.
- 212 36. Gelmini, G.B.; Gondolo, P. Ultra-cold WIMPs: relics of non-standard pre-BBN cosmologies. *JCAP* **2008**,  
213 *0810*, 002, [arXiv:astro-ph/0803.2349].
- 214 37. Visinelli, L.; Gondolo, P. Kinetic decoupling of WIMPs: analytic expressions. *Phys. Rev.* **2015**, *D91*, 083526,  
215 [arXiv:astro-ph.CO/1501.02233].
- 216 38. Waldstein, I.R.; Erickcek, A.L.; Ilie, C. Quasidecoupled state for dark matter in nonstandard thermal  
217 histories. *Phys. Rev.* **2017**, *D95*, 123531, [arXiv:astro-ph.CO/1609.05927].
- 218 39. Waldstein, I.R.; Erickcek, A.L. Comment on “Kinetic decoupling of WIMPs: Analytic expressions”. *Phys.*  
219 *Rev.* **2017**, *D95*, 088301, [arXiv:astro-ph.CO/1707.03417].
- 220 40. Dine, M.; Fischler, W. The Not So Harmless Axion. *Phys. Lett.* **1983**, *120B*, 137–141.
- 221 41. Steinhardt, P.J.; Turner, M.S. Saving the Invisible Axion. *Phys. Lett.* **1983**, *129B*, 51.

- 222 42. Turner, M.S. Coherent Scalar Field Oscillations in an Expanding Universe. *Phys. Rev.* **1983**, *D28*, 1243.
- 223 43. Scherrer, R.J.; Turner, M.S. Decaying Particles Do Not Heat Up the Universe. *Phys. Rev.* **1985**, *D31*, 681.
- 224 44. Lyth, D.H.; Stewart, E.D. Thermal inflation and the moduli problem. *Phys. Rev.* **1996**, *D53*, 1784–1798,  
225 [\[arXiv:hep-ph/hep-ph/9510204\]](#).
- 226 45. Chung, D.J.H.; Kolb, E.W.; Riotto, A. Production of massive particles during reheating. *Phys. Rev.* **1999**,  
227 *D60*, 063504, [\[arXiv:hep-ph/hep-ph/9809453\]](#).
- 228 46. Giudice, G.F.; Kolb, E.W.; Riotto, A. Largest temperature of the radiation era and its cosmological  
229 implications. *Phys. Rev.* **2001**, *D64*, 023508, [\[arXiv:hep-ph/hep-ph/0005123\]](#).
- 230 47. Moroi, T.; Randall, L. Wino cold dark matter from anomaly mediated SUSY breaking. *Nuclear Physics B*  
231 **2000**, *570*, 455–472, [\[hep-ph/9906527\]](#).
- 232 48. Fujii, M.; Hamaguchi, K. Nonthermal dark matter via Affleck-Dine baryogenesis and its detection  
233 possibility. *Phys. Rev.* **2002**, *D66*, 083501, [\[arXiv:hep-ph/hep-ph/0205044\]](#).
- 234 49. Fujii, M.; Ibe, M.; Yanagida, T. Thermal leptogenesis and gauge mediation. *Phys. Rev.* **2004**, *D69*, 015006,  
235 [\[arXiv:hep-ph/hep-ph/0309064\]](#).
- 236 50. Gelmini, G.B.; Gondolo, P. Neutralino with the right cold dark matter abundance in (almost) any  
237 supersymmetric model. *Phys. Rev.* **2006**, *D74*, 023510, [\[arXiv:hep-ph/hep-ph/0602230\]](#).
- 238 51. Gelmini, G.; Gondolo, P.; Soldatenko, A.; Yaguna, C.E. The Effect of a late decaying scalar on the neutralino  
239 relic density. *Phys. Rev.* **2006**, *D74*, 083514, [\[arXiv:hep-ph/hep-ph/0605016\]](#).
- 240 52. Acharya, B.S.; Kane, G.; Watson, S.; Kumar, P. A Non-thermal WIMP Miracle. *Phys. Rev.* **2009**, *D80*, 083529,  
241 [\[arXiv:astro-ph.CO/0908.2430\]](#).
- 242 53. Grin, D.; Smith, T.; Kamionkowski, M. Thermal axion constraints in non-standard thermal histories. *AIP*  
243 *Conf. Proc.* **2010**, *1274*, 78–84.
- 244 54. Harigaya, K.; Kawasaki, M.; Mukaida, K.; Yamada, M. Dark Matter Production in Late Time Reheating.  
245 *Phys. Rev.* **2014**, *D89*, 083532, [\[arXiv:hep-ph/1402.2846\]](#).
- 246 55. Baer, H.; Choi, K.Y.; Kim, J.E.; Roszkowski, L. Dark matter production in the early Universe: beyond the  
247 thermal WIMP paradigm. *Phys. Rept.* **2015**, *555*, 1–60, [\[arXiv:hep-ph/1407.0017\]](#).
- 248 56. Monteux, A.; Shin, C.S. Thermal Goldstino Production with Low Reheating Temperatures. *Phys. Rev.* **2015**,  
249 *D92*, 035002, [\[arXiv:hep-ph/1505.03149\]](#).
- 250 57. Reece, M.; Roxlo, T. Nonthermal production of dark radiation and dark matter. *JHEP* **2016**, *09*, 096,  
251 [\[arXiv:hep-ph/1511.06768\]](#).
- 252 58. Kane, G.L.; Kumar, P.; Nelson, B.D.; Zheng, B. Dark matter production mechanisms with a nonthermal  
253 cosmological history: A classification. *Phys. Rev.* **2016**, *D93*, 063527, [\[arXiv:hep-ph/1502.05406\]](#).
- 254 59. Erickcek, A.L. The Dark Matter Annihilation Boost from Low-Temperature Reheating. *Phys. Rev.* **2015**,  
255 *D92*, 103505, [\[arXiv:astro-ph.CO/1504.03335\]](#).
- 256 60. Kim, H.; Hong, J.P.; Shin, C.S. A map of the non-thermal WIMP. *Phys. Lett.* **2017**, *B768*, 292–298,  
257 [\[arXiv:hep-ph/1611.02287\]](#).
- 258 61. Barrow, J.D. Massive Particles as a Probe of the Early Universe. *Nucl. Phys.* **1982**, *B208*, 501.
- 259 62. Ford, L.H. Gravitational Particle Creation and Inflation. *Phys. Rev.* **1987**, *D35*, 2955.
- 260 63. Spokoiny, B. Deflationary universe scenario. *Phys. Lett.* **1993**, *B315*, 40–45, [\[arXiv:gr-qc/gr-qc/9306008\]](#).
- 261 64. Joyce, M. Electroweak Baryogenesis and the Expansion Rate of the Universe. *Phys. Rev.* **1997**,  
262 *D55*, 1875–1878, [\[arXiv:hep-ph/hep-ph/9606223\]](#).
- 263 65. Salati, P. Quintessence and the relic density of neutralinos. *Phys. Lett.* **2003**, *B571*, 121–131,  
264 [\[arXiv:astro-ph/astro-ph/0207396\]](#).
- 265 66. Profumo, S.; Ullio, P. SUSY dark matter and quintessence. *JCAP* **2003**, *0311*, 006,  
266 [\[arXiv:hep-ph/hep-ph/0309220\]](#).
- 267 67. Feng, J.L.; Rajaraman, A.; Takayama, F. SuperWIMP dark matter signals from the early universe. *Phys.*  
268 *Rev.* **2003**, *D68*, 063504, [\[arXiv:hep-ph/hep-ph/0306024\]](#).
- 269 68. Feng, J.L.; Su, S.f.; Takayama, F. SuperWIMP gravitino dark matter from slepton and sneutrino decays.  
270 *Phys. Rev.* **2004**, *D70*, 063514, [\[arXiv:hep-ph/hep-ph/0404198\]](#).
- 271 69. Pallis, C. Quintessential kination and cold dark matter abundance. *JCAP* **2005**, *0510*, 015,  
272 [\[arXiv:hep-ph/hep-ph/0503080\]](#).
- 273 70. Gomez, M.E.; Lola, S.; Pallis, C.; Rodriguez-Quintero, J. Quintessential Kination and Thermal Production  
274 of SUSY e-WIMPs. *AIP Conf. Proc.* **2009**, *1115*, 157–162, [\[arXiv:hep-ph/0809.1982\]](#).

- 275 71. Lola, S.; Pallis, C.; Tzelati, E. Tracking Quintessence and Cold Dark Matter Candidates. *JCAP* **2009**,  
276 *0911*, 017, [[arXiv:hep-ph/0907.2941](#)].
- 277 72. Lewicki, M.; Rindler-Daller, T.; Wells, J.D. Enabling Electroweak Baryogenesis through Dark Matter. *JHEP*  
278 **2016**, *06*, 055, [[arXiv:hep-ph/1601.01681](#)].
- 279 73. Artymowski, M.; Lewicki, M.; Wells, J.D. Gravitational wave and collider implications of electroweak  
280 baryogenesis aided by non-standard cosmology. *JHEP* **2017**, *03*, 066, [[arXiv:hep-ph/1609.07143](#)].
- 281 74. Redmond, K.; Erickcek, A.L. New Constraints on Dark Matter Production during Kination. *Phys. Rev.*  
282 **2017**, *D96*, 043511, [[arXiv:hep-ph/1704.01056](#)].
- 283 75. D'Eramo, F.; Fernandez, N.; Profumo, S. When the Universe Expands Too Fast: Relentless Dark Matter  
284 **2017**. [[arXiv:hep-ph/1703.04793](#)].
- 285 76. Pallis, C. Kination-dominated reheating and cold dark matter abundance. *Nucl. Phys.* **2006**, *B751*, 129–159,  
286 [[arXiv:hep-ph/hep-ph/0510234](#)].
- 287 77. Choi, K.Y.; Kim, J.E.; Lee, H.M.; Seto, O. Neutralino dark matter from heavy axino decay. *Phys. Rev.* **2008**,  
288 *D77*, 123501, [[arXiv:hep-ph/0801.0491](#)].